Sparse Polarization-Sensitive Array Optimization for Enhanced Anti-Jamming Performance

Xiangrong Wang[1], Zimeng Hu[1], Weitong Zhai[1], Maria Sabrina Greco[2], and Fulvio Gini[2]
[1]School of Electronic and Information Engineering, Beihang University, Beijing, China
[2]Department of Information Engineering, University of Pisa, Pisa, Italy
Email: {xrwang, wtzhai}@buaa.edu.cn, {maria.greco, fulvio.gini}@unipi.it

***Abstract*—Polarization-sensitive arrays are capable of enhancing anti-jamming performance by leveraging Degrees of Freedom (DoFs) in the joint spatial and polarization domain. However, existing works employ either full electromagnetic (EM) vector antennas or simple dual-polarized antennas, neglecting the flexibility in antenna polarization selection. In our previous works, an optimal sparse scalar antenna array was designed for improved adaptive beamforming. Building upon these works, this paper proposes an optimal design of sparse polarization-sensitive array in terms of maximum signal-to-interference-plus-noise ratio (MSINR). To characterize the compound impact of antenna polarization and array configuration on the SINR, we define a parameter, referred to as spatial-polarization correlation coefficient (SPCC), which is the product of spatial correlation coefficient (SCC) and polarization correlation coefficient (PCC) in the scenario of single source and single interference. The two parameters, SCC and PCC are minimized separately for optimal sparse polarimetric array design. Simulations demonstrate significant SINR improvement with optimal sparse polarimetric arrays, especially in suppressing mainlobe interferences.**

***Index Terms*—Sparse arrays, Spatial-polarization correlation coefficient, Antenna selection, Polarization selection.**

I. Introduction

Compared to scalar antenna arrays, polarization-sensitive arrays (PSAs), which are comprised of multiple electromagnetic (EM) dipoles, are capable of achieving superior anti-jamming performance attributed to the additional Degrees of Freedom (DoFs) in the polarization domain. Modern polarimetric radars are capable of transmitting waveforms in both horizontal and vertical directions and are widely used in various application fields, especially in weather detection [1], [2]. There are a few works in the literature which investigate the role of polarization played in filtering performance [3], [4]. Moreover, Li et al. verified that the polarization differences between the source and interference can be utilized for filtering and put forward a Spatial-Polarization Least Mean Square (SPNLMS) algorithm [5]. Yang et al. introduced the construction of the oblique projection spatial-frequency-polarization filter (OPSFPF) which exhibits superior performance when more processing domains are involved [6]. Mao et al. proposed a Segment Sampling Filtering (SSF) algorithm in the spatial-polarization domain based on dual-polarized arrays for suppressing mainlobe interferences [7]. However, most existing studies in the literature either use full EM vector antennas with six dipoles or simple dual-polarized antennas, overlooking the flexibility and potential DoFs in antenna polarization selection.

Although polarization-sensitive arrays are effective in interference suppression, their prohibitively high hardware cost, associated with one complete radio frequency (RF) processing chain for each dipole, hinders their practical applications. Sparse arrays, usually performed by prejudicially selecting a subset of antennas from a full dense counterpart via RF switches, present themselves as favorable solutions to reduce Size, Weight, and Power (SWaP) while preserving the full array performance [9], [10]. Some studies aim to synthesize a desired-shaped beampattern using the minimum number of antennas [11], [12], while others focus on selecting an optimal subset of antennas or beams from a large set to maximize the array gain (AG) [13], [14]. Hamza and Amin proposed a matrix completion method to integrate structured and unstructured sparse arrays [15]. Our previous work delved into a cognitive-driven MIMO array design in achieving enhanced beamforming and anti-jamming in the dynamic environment [16]–[18]. However, all these works on sparse arays are restricted to conventional scalar antennas, none of them consider the sparse array design of polarization sensitive antennas.

To fill the existing gap, we investigate the optimum design of sparse PSAs for enhanced anti-jamming performance in this work. In order to quantitatively characterize the compound impact of antenna polarization and array configuration on the output SINR of adaptive beamformers, a parameter, referred to as spatial-polarization correlation coefficient (SPCC) is defined, which is the product of spatial correlation coefficient (SCC) and polarization correlation coefficient (PCC) in the scenario of single source and single interference. The parameter SCC, which was proposed in our previous works, describes the effect of array configuration on SINR in spatial domain, while the PCC characterizes the separation between the source and the interference in the polarization domain. The optimal design of PSAs can be achieved by separately minimizing SCC and PCC. Note that although there are some works exploring the selection or reconfiguration of PSAs, they fix the antenna polarization status to either dual- or triple-polarized [19], [20], without considering the antenna polarization selection.

The main contributions of this works are summarized as follows,

- define a parameter, SPCC, to characterize the compound

The work by X. Wang is partially supported by National Natural Science Foundation of China under Grant No. U2333212 and sponsored by Beijing Nova Program No. 2022484107, No. 20240484539, by Beijing Natural Science Foundation No. L244045.

impact of antenna polarization and array configuration on the output SINR of adaptive beamforming;
- propose an optimal design of SPAs to enhance the interference suppression performance while reducing the system overhead via joint antenna and dipole selection.
- verify the effectiveness of antenna polarization selection in terms of improving anti-jamming performance.

This paper is organized as follows: Sect. II introduces the joint spatial-polarization beamforming. Sect. III proposes the optimal design of PSAs. Simulation results are presented in Sect. IV. Conclusions are drawn in Sect. V.

II. Joint Spatial-Polarization Beamforming

In this section, we first review the waveform polarization, based on which we introduce the beamforming in the joint spatial-polarization domain and derive the SPCC parameter.

A. Waveform Polarization

The electric and magnetic field of transverse electromagnetic (TEM) waves are always perpendicular to the wave propagation direction. Under far-field conditions, assuming the TEM wave propagates along the positive z-direction, the instantaneous electric field vector, denoted as $\mathbf{E}(t)$, can be decomposed into orthogonal components in the xoy-plane,

$$\mathbf{E}(t) = E_x(t)\mathbf{x} + E_y(t)\mathbf{y}, \tag{1}$$

where $E_x(t) = E_1 e^{j(2\pi f_0 t+\varphi_1)}$, $E_y(t) = E_2 e^{j(2\pi f_0 t+\varphi_2)}$, and $\mathbf{x}$ and $\mathbf{y}$ are orthonormal basis vectors in the xoy-plane.

The complex electric-field vector can then be rewritten as,

$$\hat{\mathbf{E}} = \begin{bmatrix} E_1 e^{j\varphi_1} \\ E_2 e^{j\varphi_2} \end{bmatrix} = A \begin{bmatrix} \cos\gamma \\ \sin\gamma e^{j\delta} \end{bmatrix} e^{j\varphi_1}, \tag{2}$$

where $A = \sqrt{E_1^2 + E_2^2}$ denotes the electric-field amplitude, $\gamma = \tan^{-1}(E_1/E_2)$ is the polarization auxiliary angle, and $\delta = \varphi_2 - \varphi_1$ is the polarization phase difference. The value ranges of γ and δ are $\gamma \in [0, \frac{\pi}{2}]$ and $\delta \in [0, 2\pi)$, respectively. It can be seen from Eq. (2) that the polarization information of the EM wave mainly depends on the amplitude ratio $\tan\gamma$ and the phase difference δ. For example, when $\delta = 0$ or $\delta = \pi$, the EM wave is linearly polarized (LP); when $\delta = \mp\frac{\pi}{2}$ and $\gamma = \frac{\pi}{4}$, the EM wave is circularly polarized (CP) [21].

Assume that the polarization-sensitive antenna is located at the origin of the coordinate system, and the direction of arrival (DOA) of the signal is (θ, φ), where θ and φ represent the elevation and azimuth, respectively. The signal is a fully polarized wave with polarization parameters (γ, δ), and the complex baseband signal carrying information is $g(t)$. Suppose the antenna is a full EM vector sensor, which can measure the electric field vectors in three directions and the magnetic field vectors in three directions. The polarized signal vector received by the antenna is,

$$\mathbf{s}_P(t) = \mathbf{s}_P(\theta, \varphi, \gamma, \delta)g(t), \tag{3}$$

where $\mathbf{s}_P(\theta, \varphi, \gamma, \delta)$ is defined as the steering vector in the polarization-domain, given by,

$$\begin{aligned} \mathbf{s}_P(\theta, \varphi, \gamma, \delta) &= [E_x, E_y, E_z, H_x, H_y, H_z]^T \\ &= \mathbf{D}(\varphi, \theta)\mathbf{p}(\gamma, \delta), \end{aligned} \tag{4}$$

where $\mathbf{D}(\varphi, \theta)$ is called the spatial angular position matrix, and $\mathbf{p}(\gamma, \delta)$ is called the polarization state vector, defined as,

$$\mathbf{D}(\varphi, \theta) = \begin{bmatrix} -\sin\varphi & \cos\theta\cos\varphi \\ \cos\varphi & \cos\theta\sin\varphi \\ 0 & -\sin\theta \\ \cos\theta\cos\varphi & \sin\varphi \\ \cos\theta\sin\varphi & -\cos\varphi \\ -\sin\theta & 0 \end{bmatrix}, \mathbf{p}(\gamma, \delta) = \begin{bmatrix} \cos\gamma \\ \sin\gamma \cdot e^{j\delta} \end{bmatrix}$$

It can be seen from Eq. (4) that the signal received by the polarization-sensitive antenna is related to both the polarization state and the DOA of the incident signal.

B. Joint Spatial-Polarization Beamforming

Consider a uniform linear array (ULA) where N polarization sensitive antennas are evenly arranged on the Y-axis with an inter-element spacing of d. Assuming there is an interference $j(t)$ intruding the array near the desired signal, by vectorizing the data received by all antennas across all six dipoles, the echo vector received by the PSA is expressed as,

$$\mathbf{r}(t) = \mathbf{s}g(t) + \mathbf{v}j(t) + \mathbf{n}(t), \tag{5}$$

where $\mathbf{n}(t)$ is the zero-mean complex Gaussian noise with covariance $\sigma_n^2\mathbf{I}_{6N}$, $\mathbf{s}$ and $\mathbf{v}$ are the joint spatial-polarization steering vectors of the desired signal and interference, respectively. We denote the desired signal and the interference as $(\theta_s, \varphi_s, \gamma_s, \delta_s)$ and $(\theta_j, \varphi_j, \gamma_j, \delta_j)$, respectively. The joint spatial-polarization steering vector $\mathbf{s}$ is defined as,

$$\mathbf{s} = \mathbf{s}_P(\varphi_s, \theta_s, \gamma_s, \delta_s) \otimes \mathbf{s}_s(\varphi_s, \theta_s) \tag{6}$$

where $\otimes$ represents the Kronecker product, and $\mathbf{s}_s$ is the spatial domain steering vector, given by,

$$\mathbf{s}_s = \left[1, \cdots, e^{-j(N-1)\frac{2\pi}{\lambda}d\sin\theta_s\sin\varphi_s}\right]^T, \tag{7}$$

To enhance the desired signal at the receive end, we employ the Capon beamformer to maximize output SINR, which can be expressed as,

$$\text{SINR} = \frac{P_s|\mathbf{w}_{\text{Capon}}^H\mathbf{s}|^2}{\mathbf{w}_{\text{Capon}}^H\mathbf{R}_{j+n}\mathbf{w}_{\text{Capon}}} = P_s\mathbf{s}^H\mathbf{R}_{j+n}^{-1}\mathbf{s}, \tag{8}$$

where P_s is the power of the desired signal and $\mathbf{R}_{j+n}$ denotes the interference-plus-noise covariance matrix, that is,

$$\mathbf{R}_{j+n} = P_j\mathbf{v}\mathbf{v}^H + \sigma_n^2\mathbf{I}_{6N}, \tag{9}$$

with $\mathbf{P}_j = E\{j(t)j^H(t)\}$ representing the interference power.

Applying the matrix inversion lemma to Eq. (9), the inverse matrix of $\mathbf{R}_{j+n}$ can be expressed as,

$$\begin{aligned} \mathbf{R}_{j+n}^{-1} &= (P_j\mathbf{v}\mathbf{v}^H + \sigma_n^2\mathbf{I}_{6N})^{-1} \\ &= \frac{1}{\sigma_n^2}\left(\mathbf{I}_{6N} - \frac{\text{INR}}{1 + \text{INR}\,\|\mathbf{v}\|^2}\mathbf{v}\mathbf{v}^H\right), \end{aligned} \tag{10}$$

where INR $= \frac{P_j}{\sigma_n^2}$ represents the interference-to-noise power ratio (INR). By substituting Eq. (10) into Eq. (8), the output SINR can be re-expressed into,

$$\text{SINR} = \text{SNR} \ \|\mathbf{s}\|^2 \left(1 - \chi \frac{\left|\mathbf{v}^H \mathbf{s}\right|^2}{\|\mathbf{s}\|^2 \|\mathbf{v}\|^2}\right) \tag{11}$$

where SNR $= \frac{P_s}{\sigma_n^2}$ denotes the input SNR, and $\chi = \frac{\text{INR}\|\mathbf{v}\|^2}{1+\text{INR}\|\mathbf{v}\|^2}$ is a parameter that reflects the interference intensity. Typically, in a strong interference environment where INR $\gg 1$, we have $\chi \approx 1$. Under this condition, Eq. (11) is further simplified as,

$$\text{SINR} \approx \text{SNR} \ \|\mathbf{s}\|^2 (1 - \rho), \tag{12}$$

where,

$$\rho = \frac{\left|\mathbf{v}^H \mathbf{s}\right|^2}{\|\mathbf{s}\|^2 \|\mathbf{v}\|^2} = \frac{\left|{\mathbf{v}_P}^H \mathbf{s}_P\right|^2}{\|\mathbf{s}_P\|^2 \|\mathbf{v}_P\|^2} \cdot \frac{\left|{\mathbf{v}_s}^H \mathbf{s}_s\right|^2}{\|\mathbf{s}_s\|^2 \|\mathbf{v}_s\|^2} = \rho_P \cdot \rho_s, \tag{13}$$

is defined as the spatial-polarization correlation coefficient (SPCC) between the desired signal and interference. SPCC characterizes the separation between the source and the interference in the joint spatial-polarization domain. Moreover, ρ_s and ρ_P are the spatial correlation coefficient (SCC) and the polarization correlation coefficient (PCC) between the desired signal and the interference, respectively, which are defined as,

$$\rho_s = \frac{\left|{\mathbf{v}_s}^H \mathbf{s}_s\right|^2}{\|\mathbf{s}_s\|^2 \|\mathbf{v}_s\|^2}, \ \rho_P = \frac{\left|{\mathbf{v}_P}^H \mathbf{s}_P\right|^2}{\|\mathbf{s}_P\|^2 \|\mathbf{v}_P\|^2}. \tag{14}$$

Note that the derivation of Eq. (14) utilizes the following properties of kronecker product,

$$\|\mathbf{s}\|^2 = \|\mathbf{s}_P \otimes \mathbf{s}_s\|^2 = \|\mathbf{s}_P\|^2 \|\mathbf{s}_s\|^2, \tag{15}$$

$$\|\mathbf{v}\|^2 = \|\mathbf{v}_P \otimes \mathbf{v}_s\|^2 = \|\mathbf{v}_P\|^2 \|\mathbf{v}_s\|^2, \tag{16}$$

$$\mathbf{v}^H \mathbf{s} = (\mathbf{v}_P \otimes \mathbf{v}_s)^H (\mathbf{s}_P \otimes \mathbf{s}_s) = (\mathbf{v}_P^H \mathbf{s}_P)(\mathbf{v}_s^H \mathbf{s}_s). \tag{17}$$

Substituting Eq. (14) into Eq. (12), the maximum array output SINR can be expressed in terms of ρ_s and ρ_P as,

$$\text{SINR} = \text{SNR} \ \|\mathbf{s}\|^2 (1 - \rho_P \cdot \rho_s). \tag{18}$$

Combining Eqs. (12) and (18), it can be concluded that the beamforming output SINR monotonically decreases with the SPCC ρ between the desired signal and interference, or equivalently, with the spatial correlation coefficient ρ_s and the polarization correlation coefficient ρ_P. Additionally, the norm of the source steering vector $\|\mathbf{s}\|^2$ indicates the array gain against white noise and more antennas with more dipoles underscores a larger gain.

III. Sparse Polarization-Sensitive Array Design

In this section, we consider the sparse PSA design via joint antenna and polarization selection, aiming to reduce the cost while enhancing the output SINR. Specifically, consider selecting a subset of K antennas from an N-element full ULA and connecting them to the RF-chains for processing. Additionally, the polarization characteristics of the selected antennas are jointly optimized via dipole selection to further improve the filtering performance. To this end, we introduce an antenna selection vector $\mathbf{z} \in \{0,1\}^N$ and a dipole selection vector $\mathbf{x} \in \{0,1\}^6$, with an entry of "1" indicating the corresponding antenna or dipole selected, otherwise discarded. Consequently, ρ_s, ρ_P and $||\mathbf{s}||^2$ of a selected sparse PSA can be expressed as,

$$\rho_s = \frac{\left|{\mathbf{v}_s}^H \text{diag}(\mathbf{z}) \mathbf{s}_s\right|^2}{K^2}, \tag{19}$$

$$\rho_P = \frac{|{\mathbf{v}_P}^H \text{diag}(\mathbf{x}) \mathbf{s}_P|^2}{{\mathbf{v}_P}^H \text{diag}(\mathbf{x}) \mathbf{v}_P \bullet {\mathbf{s}_P}^H \text{diag}(\mathbf{x}) \mathbf{s}_P}, \tag{20}$$

$$||\mathbf{s}||^2 = K \mathbf{s}_P^H \text{diag}(\mathbf{x}) \mathbf{s}_P. \tag{21}$$

The SINR maximization problem can be decomposed into two independent subproblems: antenna selection and polarization selection. For antenna selection, since the SINR monotonically decreases with respect to ρ_s, the objective is to minimize ρ_s in terms of antenna selection $\mathbf{z}$. Once the optimal array configuration is determined, the polarization selection is then optimized to maximize the SINR in the second step.

A. Antenna Selection

As previously discussed, the optimal design of the array geometry necessitates minimizing the SCC ρ_s by solving the following optimization problem,

$$(Q_1) \ \min_{\mathbf{z}} \quad \rho_s, \tag{22a}$$

$$\text{s.t.} \quad \mathbf{1}^T \mathbf{z} = K, \tag{22b}$$

$$\mathbf{z} \in \{0,1\}^N. \tag{22c}$$

The constraint $\mathbf{1}^T \mathbf{z} = K$ ensures that exactly K antennas are selected. Substituting Eq. (19), the objective function ρ_s can be rewritten as,

$$\rho_s = \frac{\mathbf{z}^T \mathbf{R}_s \mathbf{z}}{K^2}, \tag{23}$$

where $\mathbf{R}_s = \text{diag}(\mathbf{v}_s^H) \mathbf{s}_s \cdot \mathbf{s}_s^H \text{diag}(\mathbf{v}_s)$. It is obvious that $\mathbf{R}_s$ is a positive semi-definite matrix, which ensures that the numerator $\mathbf{z}^T \mathbf{R}_s \mathbf{z}$ is a real number. Consequently, we have,

$$\mathbf{z}^T \mathbf{R}_s \mathbf{z} = \mathbf{z}^T \text{real}(\mathbf{R}_s) \mathbf{z}. \tag{24}$$

Let $\overline{\mathbf{R}}_s = \text{real}(\mathbf{R}_s)$, then we can transform problem (Q_1) into the real domain as follows,

$$(Q_2) \ \min_{\mathbf{z}} \quad \mathbf{z}^T \overline{\mathbf{R}}_s \mathbf{z}, \tag{25a}$$

$$\text{s.t.} \quad \mathbf{1}^T \mathbf{z} = K, \tag{25b}$$

$$\mathbf{z} \in \{0,1\}^N. \tag{25c}$$

In (Q_2), since $\mathbf{R}_s$ is positive semi-definite, $\overline{\mathbf{R}}_s$ is also positive semi-definite. Thus, the objective function in (25a) is convex. However, the binary constraint (25c) is non-convex. To resolve this, we relax it into a box constraint and iteratively enhance sparsity using the re-weighted l_1 method [22]. In the $(k+1)$-th iteration, the optimization problem is given by,

$$(Q_3) \ \min_{\mathbf{z}} \quad \mathbf{z}^T \overline{\mathbf{R}}_s \mathbf{z} + \beta_0 \mathbf{u}_{(k)}^T \mathbf{z}, \tag{26a}$$

$$\text{s.t.} \quad \mathbf{1}^T \mathbf{z} = K, \tag{26b}$$

$$0 \le \mathbf{z} \le 1, \tag{26c}$$

where β_0 is a preset constant, $\mathbf{u}_{(k)}^T = \frac{1}{\mathbf{z}_{(k)}+\varepsilon_0}$ is the weighting vector used to promote the sparsity of $\mathbf{z}$, $\mathbf{z}_{(k)}$ is the solution to the k-th iteration, and ε_0 is a small positive constant.

B. Polarization Selection

We further consider optimizing the antenna polarization via dipole selection to maximize the SINR. Under the optimized array configuration, substituting Eqs. (20) and (21) into Eq. (12), we can express the maximum output SINR in Eq. (18) as a function of variable $\mathbf{x}$ as follows,

$$\begin{aligned} f(\mathbf{x}) =& \text{SNR} \cdot K(\mathbf{s}_P^H \text{diag}(\mathbf{x})\mathbf{s}_P - \rho_s \cdot \frac{|\mathbf{v}_P{}^H \text{diag}(\mathbf{x})\mathbf{s}_P|^2}{\mathbf{v}_P{}^H \text{diag}(\mathbf{x})\mathbf{v}_P}) \\ =& \text{SNR} \cdot K(-\rho_s \frac{\mathbf{x}^T \text{diag}(\mathbf{v}_P^H)\mathbf{s}_P \mathbf{s}_P^H \text{diag}(\mathbf{v}_P)\mathbf{x}}{\mathbf{x}^T \text{diag}(\mathbf{v}_P^H)\mathbf{v}_P} \\ &+ \mathbf{x}^T \text{diag}(\mathbf{s}_P^H)\mathbf{s}_P) \end{aligned} \tag{27}$$

Define $\mathbf{R}_P = \text{diag}(\mathbf{v}_P^H)\mathbf{s}_P\mathbf{s}_P^H\text{diag}(\mathbf{v}_P)$, $\overline{\mathbf{R}}_P = \text{real}(\mathbf{R}_P)$ $\bar{\mathbf{s}}_P = \text{diag}(\mathbf{s}_P^H)\mathbf{s}_P$, and $\bar{\mathbf{v}}_P = \text{diag}(\mathbf{v}_P^H)\mathbf{v}_P$, Eq. (27) can be rewritten as,

$$f(\mathbf{x}) = \text{SNR} \cdot K\left(\mathbf{x}^T \bar{\mathbf{s}}_P - \rho_s \frac{\mathbf{x}^T \overline{\mathbf{R}}_P \mathbf{x}}{\mathbf{x}^T \bar{\mathbf{v}}_P}\right). \tag{28}$$

In this work, we assume that K antennas share the same polarization configuration, where each dipole type needs a dedicated RF channel. While increasing the number of polarization channels can enhance system performance, it also significantly raises hardware costs. Thus, we aim at maximizing SINR while limiting the number of selected dipoles through a penalty term. The optimization problem for polarization selection can be formulated as,

$$(Q_4) \quad \max_{\mathbf{x}} \quad f(\mathbf{x}), \tag{29a}$$

$$\text{s.t.} \quad \mathbf{1}^T\mathbf{z} = L, \tag{29b}$$

$$\text{s.t.} \quad \mathbf{x} \in \{0,1\}, \tag{29c}$$

where the constraint $\mathbf{1}^T\mathbf{z} = L$ ensures that exactly L dipoles for each polarized antenna are selected.

In (Q_4), since the first term of $f(\mathbf{x})$ is linear and the second term is convex, the entire objective function is convex. The non-convexity of (Q_4) stems solely from the binary constraint (29c). Thus, we can iteratively solve (Q_4) using the same re-weighted l_1 approach as in solving (Q_3).

IV. Simulation Results

In the simulation, we consider a full array composed of $N = 16$ elements with half-wavelength inter-element spacing and select $K = 8$ antennas from it to form the sparse beamformer. Suppose there is one target and one interference in the observation region, their spatial-polarization parameters are denoted as $(\theta_s = 35°, \varphi_s = 90°, \gamma_s = 45°, \delta_s = 0)$ and $(\theta_j = 30°, \varphi_j = 90°, \gamma_j = 81°, \delta_j = 0°)$, respectively, with the SNR of the target being -20dB and the INR of the interference being 30dB.

In this scenario, we jointly optimize antenna and polarization selection applying the proposed method in Section III under the constraints of selecting $L = 2, 3, 4, 5$ dipoles, respectively. The optimum antenna-polarization configurations are depicted in Fig. 1. As derived in Sect. III, antenna selection and polarization selection can be regarded as two independent subproblems. Hence, the optimum array configuration remains identical under the constraints of different selected dipole number, while antenna polarization is different.

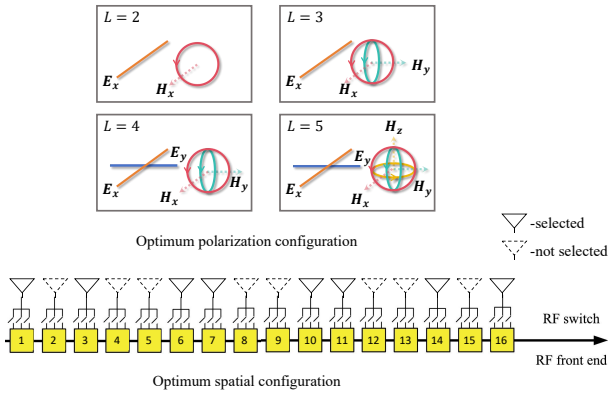

Fig. 1: Optimum PSA, where E_x, E_y, E_z denote electric and H_x, H_y, H_z magnetic dipoles along x, y and z axis.

To demonstrate the necessity of polarization selection, we exhaustively evaluated the output SINR for all possible dipole compositions under the optimal array configuration in the cases of $L = 2, 3, 4, 5$, respectively. The results are shown in Fig. 2. Taking $L = 2$ as an example, we enumerate all $C_6^2 = 15$ possible cases of selecting 2 dipoles from 6. The optimal polarization selected by our proposed method is highlighted in the cyan circles. It can be deduced from the results that different polarization selections have a significant impact on beamforming performance, and the proposed algorithm is capable of efficiently selecting the optimal polarization status under arbitrary dipole number constraints.

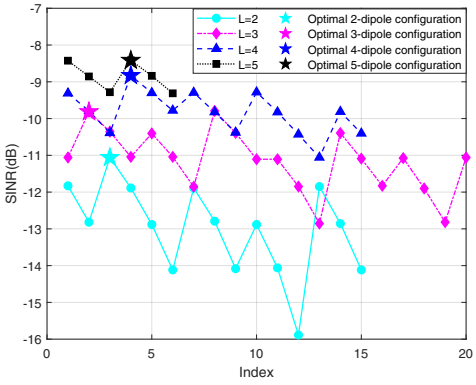

Fig. 2: SPACE SINR performance in all dipole selections.

To investigate the influence of array configuration and dipole selection on SINR performance, we compared three array configurations, as shown in Fig. 3a: (1) the optimized array with joint antenna-polarization selection, (2) the 8-antenna ULA with half-wavelength inter-element spacing, and (3) the random array containing the first and 16th antennas to

maintain the maximum aperture. The signal is fixed ($\theta_s = 35°, \varphi_s = 90°, \gamma_s = 45°, \delta_s = 0$) and the interference polarization parameters are ($\gamma_j = 81°, \delta_j = 0°$). In Fig. 3a, the optimized array configuration, selected via angle-dependent optimization, exhibits significantly improved SINR compared to both uniform and random arrays. This enhancement primarily manifests in narrower null width and improved spatial resolution. Moreover, we can find from Fig. 3b that polarization optimization plays a critical role in suppressing mainlobe interferences, where the optimized configuration achieves at least 2dB SINR improvement over random dipole selection. This observation further emphasizes the necessity of polarization optimization.

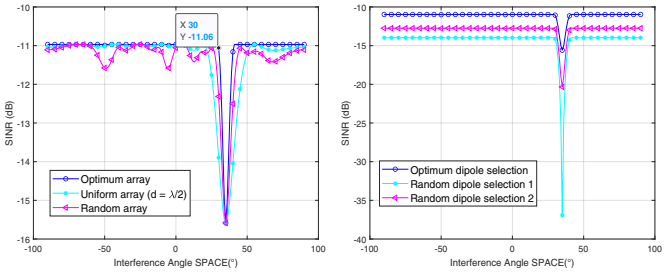

(a) Fixed optimal dipole selection (b) Fixed optimal antenna selection

Fig. 3: Performance of PSA versus different interference angle.

V. Conclusions

This paper proposed an optimal sparse polarization-sensitive array design to improve anti-jamming performance. The sparse SPA was optimized in terms of minimizing the spatial-polarization correlation coefficient (SPCC), which measured the compound impact of array configuration and antenna polarization on output SINR. The optimal array configuration and antenna polarization were designed via selecting a subset of antennas and a subset of dipoles to minimize the spatial correlation coefficient and polarization correlation coefficient. The numerical results showed that the proposed sparse SPA can fully deploy the DoFs in the joint spatial and polarization domain, thus improving the anti-jamming performance, especially in suppressing mainlobe interferences with reduced hardware cost compared to full electromagnetic vector arrays.

References

[1] W. Shao, Y. Hu, Z. Lai, Y. Zhang and X. Jiang, "Rain Rate Retrieval Algorithm for Dual-Polarized Sentinel-1 SAR in Tropical Cyclone," in IEEE Geoscience and Remote Sensing Letters, vol. 20, pp. 1-5, 2023, Art no. 4011405.

[2] H. Kikuchi, Y. Hobara and T. Ushio, "Time-Altitude Variation of 30-Second-Update Full Volume Scan Data for Summer Convective Storms Observed With X-Band Dual Polarized Phased Array Weather Radar," in IEEE Access, vol. 12, pp. 104333-104343, 2024.

[3] Y. Zhang, W. Yang, Q. Xue, J. Huang and W. Che, "Broadband Dual-Polarized Differential-Fed Filtering Antenna Array for 5G Millimeter-Wave Applications," in IEEE Transactions on Antennas and Propagation, vol. 70, no. 3, pp. 1989-1998, March 2022.

[4] W. Zhao, H. Jin, W. Wang, W. Yu, K. -S. Chin and G. Q. Luo, "High-Gain Dual-Polarized Millimeter-Wave Patch Filtenna Array," in IEEE Antennas and Wireless Propagation Letters, vol. 23, no. 4, pp. 1361-1365, April 2024.

[5] F. Li, T. Lyu and H. Zhang, "A Joint Spatial-Polarization Normalized LMS Based on Circular Array," 2021 6th International Conference on Intelligent Computing and Signal Processing (ICSP), Xi'an, China, 2021, pp. 1321-1325.

[6] Y. Yang, X. Mao, Y. Hou and J. Geng, "A Two-Step Method for Ionospheric Clutter Mitigation for HFSWR With Two-Dimensional Dual-Polarized Received Array," in IEEE Access, vol. 8, pp. 105903-105913, 2020.

[7] Y. Mao and J. Meng, "Spatial-Polarization Domain Joint Filtering Under Interference Polarization Agility," 2024 4th International Conference on Electronics, Circuits and Information Engineering (ECIE), Hangzhou, China, 2024, pp. 475-480.

[8] R. Liu, D. Xu, B. Jiu, Y. Fan, Y. Zhang and H. Liu, "Multi-target high-resolution DOA estimation based on sparse reconstruction for frequency agility radar," IET International Radar Conference (IRC 2023), Chongqing, China, 2023, pp. 1420-1425.

[9] X. Wang, W. Zhai, X. Wang, M. Amin and A. Zoubir, "Wideband Near-Field Integrated Sensing and Communications: A hybrid precoding perspective," in IEEE Signal Processing Magazine, vol. 42, no. 1, pp. 88-105, Jan. 2025.

[10] X. Wang, W. Zhai, X. Wang, M. G. Amin and K. Cai, "Wideband Near-Field Integrated Sensing and Communication With Sparse Transceiver Design," in IEEE Journal of Selected Topics in Signal Processing, vol. 18, no. 4, pp. 662-677, May 2024

[11] X. Zhang and T. Gu, "Synthesis of Sparse Linear Arrays via Low-Rank Hankel Matrix Completion," in IEEE Transactions on Antennas and Propagation, vol. 72, no. 12, pp. 9522-9527, Dec. 2024.

[12] W. T. Li, J. L. Wan, Y. Q. Hei and X. W. Shi, "Efficient Two-Stage Beampattern Synthesis Against Interference for Sparse Linear Array Design," in IEEE Antennas and Wireless Propagation Letters, vol. 23, no. 7, pp. 2205-2209, July 2024.

[13] J. Zhang, X. Mao, M. Zhang, J. Hirokawa and Q. H. Liu, "Synthesis of Thinned Planar Arrays Based on Precoded Subarray Structures," in IEEE Antennas and Wireless Propagation Letters, vol. 22, no. 1, pp. 44-48, Jan. 2023.

[14] Y. Liu, T. Huang, F. Liu, D. Ma, W. Huangfu and Y. C. Eldar, "Next-Generation Multiple Access for Integrated Sensing and Communications," in Proceedings of the IEEE, vol. 112, no. 9, pp. 1467-1496, Sept. 2024.

[15] S. A. Hamza and M. G. Amin, "Sparse array design for maximizing the signal-to-interference-plus-noise-ratio by matrix completion," Digit. Signal Process., vol. 105, 2020, Art. no. 102678.

[16] X. Wang, M. Amin and X. Cao, "Analysis and Design of Optimum Sparse Array Configurations for Adaptive Beamforming," in IEEE Transactions on Signal Processing, vol. 66, no. 2, pp. 340-351, 15 Jan.15, 2018.

[17] X. Wang, C. P. Tan, Y. Wang and X. Wang, "Defending UAV Networks Against Covert Attacks Using Auxiliary Signal Injections," in IEEE Transactions on Automation Science and Engineering, vol. 22, pp. 8805-8817, 2025.

[18] X. Wang, J. Huang, X. Wang, T. Huang and M. Amin, "Optimal Sparse Array Design for Airborne Weather Radar With Integrated Communications," in IEEE Transactions on Aerospace and Electronic Systems.

[19] Y. Sun, J. Xie, C. Han, L. Wang and M. Tao, "Array Element Selection Strategies for Interference Suppression in Reconfigurable Tripole Antenna Array Systems," in IEEE Transactions on Vehicular Technology, vol. 72, no. 1, pp. 557-572, Jan. 2023.

[20] Y. Sun, J. Xie, C. Han, L. Wang, and M. Tao, "A polarization-sensitive array reconfiguration technique resorting to antenna selection for navigation interference mitigation," Digital Signal Processing, vol. 129, 2022, Art. no. 103661. [Online]. Available: https://doi.org/10.1016/j.dsp.2022.103661.

[21] D. Bu and S. -W. Qu, "Millimeter-Wave Endfire Circularly Polarized Phased Array With Wideband Wide-Angle Scanning," in IEEE Transactions on Antennas and Propagation, vol. 72, no. 10, pp. 7644-7650, Oct. 2024.

[22] W. Zhai, X. Wang, M. S. Greco and F. Gini, "Joint Optimization of Sparse FDAs for Time Invariant Transmit Beampattern Synthesis," in IEEE Signal Processing Letters, vol. 29, pp. 110-114, 2022.